

# Analysis of (n+1) and n-parton contributions for computing QCD jet cross sections in the local analytic subtraction scheme

**Bakar Chargeishvili,<sup>a,\*</sup> Giuseppe Bevilacqua,<sup>b</sup> Adam Kardos,<sup>c,d</sup> Sven-Olaf Moch<sup>a</sup> and Zoltán Trócsányi<sup>d</sup>**

<sup>a</sup>*Universität Hamburg, II. Institute for Theoretical Physics,  
Luruper Chaussee 149, 22761 Hamburg, Germany*

<sup>b</sup>*Institute of Nuclear and Particle Physics, NCSR "Demokritos", 15341 Agia Paraskevi, Greece*

<sup>c</sup>*University of Debrecen, Faculty of Science and Technology, Department of Experimental Physics, 4010,  
Debrecen, PO Box 105, Hungary*

<sup>d</sup>*Institute for Theoretical Physics, ELTE Eötvös Loránd University, Pázmány Péter sétány 1/A,  
H-1117 Budapest, Hungary*

*E-mail: [bakar.chargeishvili@desy.de](mailto:bakar.chargeishvili@desy.de), [bevilacqua@inp.demokritos.gr](mailto:bevilacqua@inp.demokritos.gr),  
[kardos.adam@science.unideb.hu](mailto:kardos.adam@science.unideb.hu), [sven-olaf.moch@desy.de](mailto:sven-olaf.moch@desy.de),  
[zoltan.trocsanyi@cern.ch](mailto:zoltan.trocsanyi@cern.ch)*

We analyze and implement the Local Analytic Sector Subtraction (LASS) scheme for handling infrared singularities in next-to-next-to-leading order (NNLO) calculations in perturbative QCD. We examine the key aspects of the scheme including sector function construction, singular limit parametrization, subtraction counterterm derivation, and integration techniques. As a proof-of-concept, we numerically implement LASS for the process  $e^+e^- \rightarrow 3$  jets. In this study we examine the limiting behavior of subtraction terms for real-virtual contribution and explicitly demonstrate the pole cancellation of the double-virtual contribution. Differential cross sections are computed for several event shape observables, showing the stability and efficiency of LASS scheme. This work lays the foundation for developing an automated tool for NNLO QCD calculations using this promising scheme.

*Loops and Legs in Quantum Field Theory (LL2024)  
14-19, April, 2024  
Wittenberg, Germany*

---

\*Speaker

## 1. Introduction

Precise theoretical predictions are crucial for interpreting collider data and testing the Standard Model. Next-to-next-to-leading order (NNLO) accuracy in QCD is now needed for many key processes. However, at NNLO, handling the infrared divergences from soft and collinear radiation is very challenging. Several approaches have been developed to treat these singularities at NNLO, including slicing methods [1, 2], non-local subtraction schemes [3, 4], and local subtraction methods like antenna subtraction [5, 6], CoLoRFulNNLO [7–9], nested soft-collinear subtraction [10] and the recently proposed Local Analytic Sector Subtraction (LASS) [11–13]. LASS aims to provide a fully local and analytic subtraction framework that can be implemented numerically within any existing code, using sector decomposition of the phase space and flexible parametrizations of singular limits to derive counterterms that can be integrated analytically. In this work, we implement LASS and apply it to the process  $e^+e^- \rightarrow 3$  jets as a proof-of-concept. We analyze the theoretical framework in depth, perform rigorous checks of the counterterms, and compute differential distributions for event shape observables.

## 2. Local Analytic Sector Subtraction at NNLO

The NNLO correction to a cross section schematically takes the form:

$$d\sigma^{\text{NNLO}} = \int d\Phi_n VV \delta_n(X) + \int d\Phi_{n+1} RV \delta_{n+1}(X) + \int d\Phi_{n+2} RR \delta_{n+2}(X) \quad (1)$$

Here  $VV$ ,  $RV$  and  $RR$  denote the double-virtual, real-virtual and double-real squared matrix elements, and  $\delta_n(X)$  fixes the observable  $X$  at its value for  $n$ -body kinematics. To numerically integrate each term, we must either eliminate or regulate all singularities. LASS achieves this by adding and subtracting counterterms: [replace sub with reg for regularized]

$$RR_{\text{sub}}(X) \equiv RR \delta_{n+2}(X) - K^{(1)} \delta_{n+1}(X) - \left( K^{(2)} - K^{(12)} \right) \delta_n(X), \quad (2)$$

$$RV_{\text{sub}}(X) \equiv \left( RV + I^{(1)} \right) \delta_{n+1}(X) - \left( K^{(\text{RV})} + I^{(12)} \right) \delta_n(X), \quad (3)$$

$$VV_{\text{sub}}(X) \equiv \left( VV + I^{(2)} + I^{(\text{RV})} \right) \delta_n(X). \quad (4)$$

$K^{(1)}$  is a counterterm that accounts for the single unresolved singularities,  $K^{(2)}$  accounts for the double unresolved singularities, and  $K^{(12)}$  is introduced to avoid double counting by removing the overlap between  $K^{(1)}$  and  $K^{(2)}$ . At RV level there is still a possibility to introduce an additional subtraction term  $K^{(\text{RV})}$  which deals with the phase-space singularities of RV contribution. So in total one needs 4 kinds of subtraction terms. Then those subtraction terms are integrated analytically over the factorized singular regions of the radiation phase spaces and the integrated versions of those subtraction terms are then added back. They are defined as:

$$\begin{aligned} I^{(1)} &\equiv \int d\Phi_{\text{rad}} K^{(1)}, & I^{(2)} &\equiv \int d\Phi_{\text{rad},2} K^{(2)}, \\ I^{(12)} &\equiv \int d\Phi_{\text{rad}} K^{(12)}, & I^{(\text{RV})} &\equiv \int d\Phi_{\text{rad}} K^{(\text{RV})}, \end{aligned} \quad (5)$$

where  $\Phi_{\text{rad}}$  parametrizes the phase-space of the single unresolved radiation and  $\Phi_{\text{rad},2}$  - the phase-space of the double unresolved radiation. To construct the counterterms, LASS partitions the phase space into sectors containing a minimal set of singularities using sector functions  $W_{abcd}$  defined in Refs. [11, 13], see also Ref. [14] in these proceedings.

Various singular projectors  $S_i, C_{ij}$  etc. are defined to parametrize different unresolved configurations. The counterterms are built by applying these projectors to the matrix element in each sector. Integrating the counterterms over the unresolved phase space is a key aspect of LASS. Flexible mappings of the phase space are used to factorize the integrals into a radiation part and a Born-level part. To this end the Catani-Seymour final-state mapping [15] is being used. This allows the counterterms to be analytically integrated over the radiation variables, yielding expressions that can be added back to the singular contributions in Eqs. (2)- (4).

### 3. Validation and results for $e^+e^- \rightarrow 3$ jets

As a proof-of-concept, we implemented the LASS scheme for the process  $e^+e^- \rightarrow 3$  jets. At NNLO, this involves the subprocesses:

$$RR : \quad e^+e^- \rightarrow q\bar{q}q\bar{q}g, \quad e^+e^- \rightarrow q\bar{q}r\bar{r}g, \quad e^+e^- \rightarrow q\bar{q}ggg, \quad (6)$$

$$RV : \quad e^+e^- \rightarrow q\bar{q}q\bar{q}, \quad e^+e^- \rightarrow q\bar{q}r\bar{r}, \quad e^+e^- \rightarrow q\bar{q}gg, \quad (7)$$

$$VV : \quad e^+e^- \rightarrow q\bar{q}g, \quad (8)$$

where the notation  $q$  and  $r$  is used to distinguish between quarks of different flavors. The processes in Eq. (6) involve only tree-level kinematics and helicity amplitudes, from which the squared matrix elements can be constructed using the results in Refs. [16–18]. The processes in Eq. (7) contain one-loop virtual corrections, and their matrix elements can be constructed using the method described in Ref. [19]. Finally, the process in Eq. (8) involves two-loop virtual corrections, and the corresponding matrix element can be found in Refs. [20, 21].

The integration over physical phase space is managed using an in-house implementation of the VEGAS+ algorithm [22].

#### 3.1 Pole cancellation and limiting behavior

As a first check, we verified the pole structure of the  $VV$  contribution by comparing the  $\epsilon$  expansion of  $I^{(2)} + I^{(RV)}$  with the known singularities of the two-loop virtual correction. We found perfect agreement.

Next, we studied the limiting behavior of the  $RV$  counterterms in all singular regions of phase space. Since  $K^{(RV)}$  is designed to cancel the phase-space singularities of  $RV$ , and  $I^{(12)}$  cancels the singularities of  $I^{(1)}$ , it is sufficient to examine their respective ratios in the singular limits appearing in the  $K^{(RV)}$  term. This has been done for each individual subprocess listed in Eq. (7). The  $e^+e^- \rightarrow q\bar{q}q\bar{q}$  process features a total of 4 singular limits,  $e^+e^- \rightarrow q\bar{q}r\bar{r}$  features 2, and  $e^+e^- \rightarrow q\bar{q}gg$  features 7 singular limits. For illustration purposes, in this proceedings we present plots obtained for the real virtual and double virtual processes with four equal flavour quarks in the final state. Our results for the other final states are very similar.

The results for the ratios of  $I^{(1)}$  and  $I^{(12)}$  pair and  $RV$  and  $K^{(RV)}$  pair for  $e^+e^- \rightarrow q\bar{q}q\bar{q}$  contribution are plotted in Fig. 1. The precise way of taking these limits together with the definition of the parameter  $\lambda$  that controls the limit is described in the contribution [14] to these proceedings. On these plots, the absolute value of the numbers read from the vertical axis indicates the number of digits of accuracy with which the ratio matches unity and the notation " $\lim_P$ " means that we are approaching that particular limit. For example, " $\lim_{C_{ijk}}$ " corresponds to the case when partons  $i$ ,  $j$ , and  $k$  become collinear.

### 3.2 Technical cut and event shape distributions

Making a step closer towards physical predictions, we computed computed differential distributions for several event shape observables. For this purpose, we choose four event shape observables typically studied in  $e^+e^- \rightarrow 3$  jet processes [23, 24]. The observables of our choice are:  $\tau$ -parameter (thrust),  $C$ -parameter, Energy-energy correlation, Jet-cone energy fraction. These observables are chosen because they provide complementary information about the event topology and the dynamics of the final-state particles, allowing for a comprehensive study of the underlying QCD processes. In this study we use the definitions taken from [23].

When computing such distributions, due to the finite precision of representing real numbers on the computer, one always have to introduce a technical cut parameter  $y_{\min}$  on the phase space to avoid numerical instabilities in the deep IR regions. Similarly to Ref. [25] we are using the following cut to exclude the unstable regions:

$$y_{\min} = \min_{i,j} \frac{S_{ij}}{s}, \quad (9)$$

To investigate the impact of this cut we perform the following study: We set the initial value of  $y_{\min}$  to  $10^{-4}$  and gradually decrease it in small intervals until it reaches to  $10^{-10}$ . For each value of  $y_{\min}$ , we perform the Monte Carlo integration by generating  $10^7$  phase-space points and optimizing the grid 40 times. After every iteration, we calculate a new estimate of the cross-section. Once all 40 iterations are completed, we plot the first moment of the thrust distribution as a function of the technical cut  $\langle \tau \rangle(y_{\min})$ . To gain further insights, we combine the results of these 40 independent estimates in each bin using two methods. First, we calculate the average of the estimates. Second, we calculate the weighted average, where the inverse values of the mean squared uncertainties are used as weights. This latter method effectively gives preference to more stable integration iterations with smaller uncertainties. The results of this study are depicted in Fig. 2.

We observe that in all studied cases a very good saturation is achieved at the value  $y_{\min} = 10^{-8}$ . We also considered the different formulations of  $y_{\min}$  and for  $RV$  contribution no significant effect was found. Hence, for the subsequent studies we fix the value of  $y_{\min}$  as defined in Eq. (9) to  $10^{-8}$ .

Next we computed the distributions of the event shape variables by taking into account the regularized real-virtual contributions. To perform this study, we utilized the integration grid obtained in the previous section. To accelerate the speed of the calculation, the integration was performed 200 times in parallel with different random number seeds, each integrating over  $10^7$  events. This means that in every bin of each event shape observable, we have 200 independent estimates. We combine these estimates using weighted averages described previously, effectively

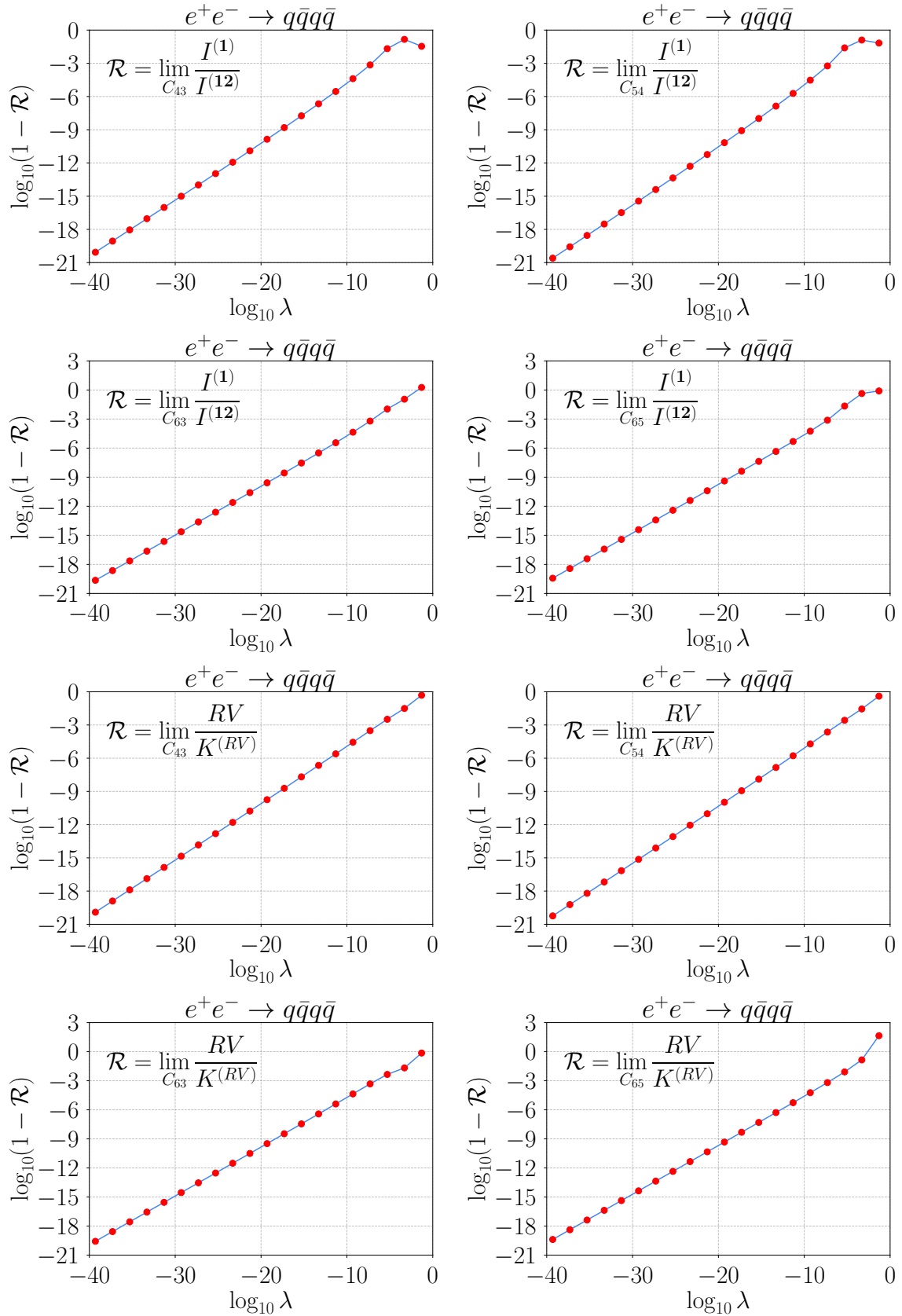


**Figure 1:** Limiting behavior of the ratio between  $I^{(1)}$  and  $I^{(12)}$  terms (top row) and  $RV$  and  $K^{(RV)}$  terms (bottom row) in various singular limits for the one-loop correction to  $e^+e^- \rightarrow q\bar{q}q\bar{q}$  contribution. Each plot corresponds to a different singular limit, as indicated on the respective plot.

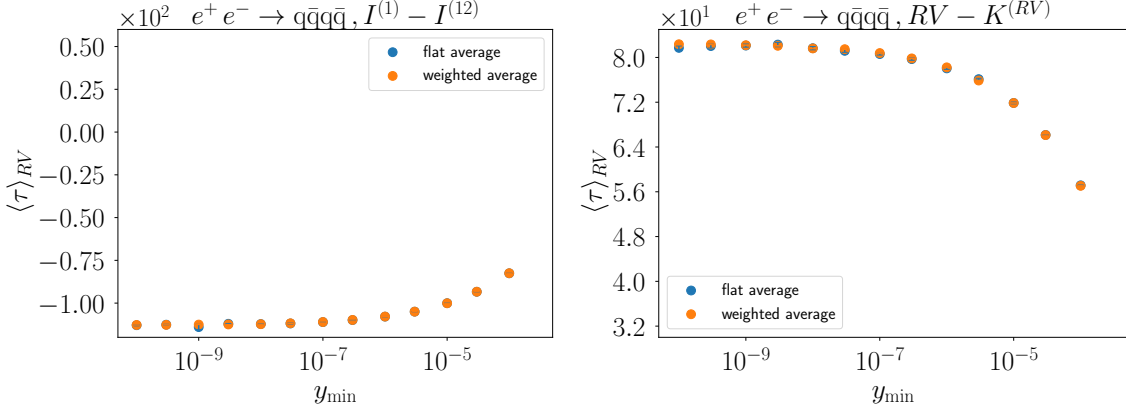


**Figure 2:** The saturation plots of  $I^{(1)} - I^{(12)}$  (to the left) and  $RV - K^{(RV)}$  (to the right) contributions to the mean value of the thrust distribution by the process  $e^+e^- \rightarrow q\bar{q}q\bar{q}$ .

accumulating the statistics of  $2 \times 10^9$  events. The results are depicted in Figs. 3 - 4. As demonstrated in all cases we observe the good numeric stability.

#### 4. Conclusions

We presented a proof-of-concept implementation of the RV and VV contributions regularized according to the LASS scheme for the NNLO corrections to  $e^+e^- \rightarrow 3$  jets. Explicit pole cancellation was demonstrated for the VV contribution. We have demonstrated that the counterterms correctly approximate the matrix elements in all IR limits. We computed differential distributions of event shape variables and found our predictions stable against variations of the technical cut. This proof-of-concept study lays the groundwork for developing LASS into a general tool for NNLO calculations. Future work will focus on optimizing the phase-space treatment, incorporating initial-state radiation and massive partons, and automating the set-up. The LASS scheme is a promising method that could substantially simplify and speed up precise predictions for collider observables in the coming years.

#### 5. Acknowledgements

A.K. is supported by the UNKP-21-Bolyai+ New National Excellence Program of the Ministry for Innovation and Technology from the source of the National Research, Development and Innovation Fund. A.K. also kindly acknowledges further financial support from the Bolyai Fellowship programme of the Hungarian Academy of Sciences. G.B is supported by the Hellenic Foundation for Research and Innovation (H.F.R.I.) under the "2nd Call for H.F.R.I. Research Projects to support Faculty Members & Researchers" (Project Number: 02674 HOCTools-II).

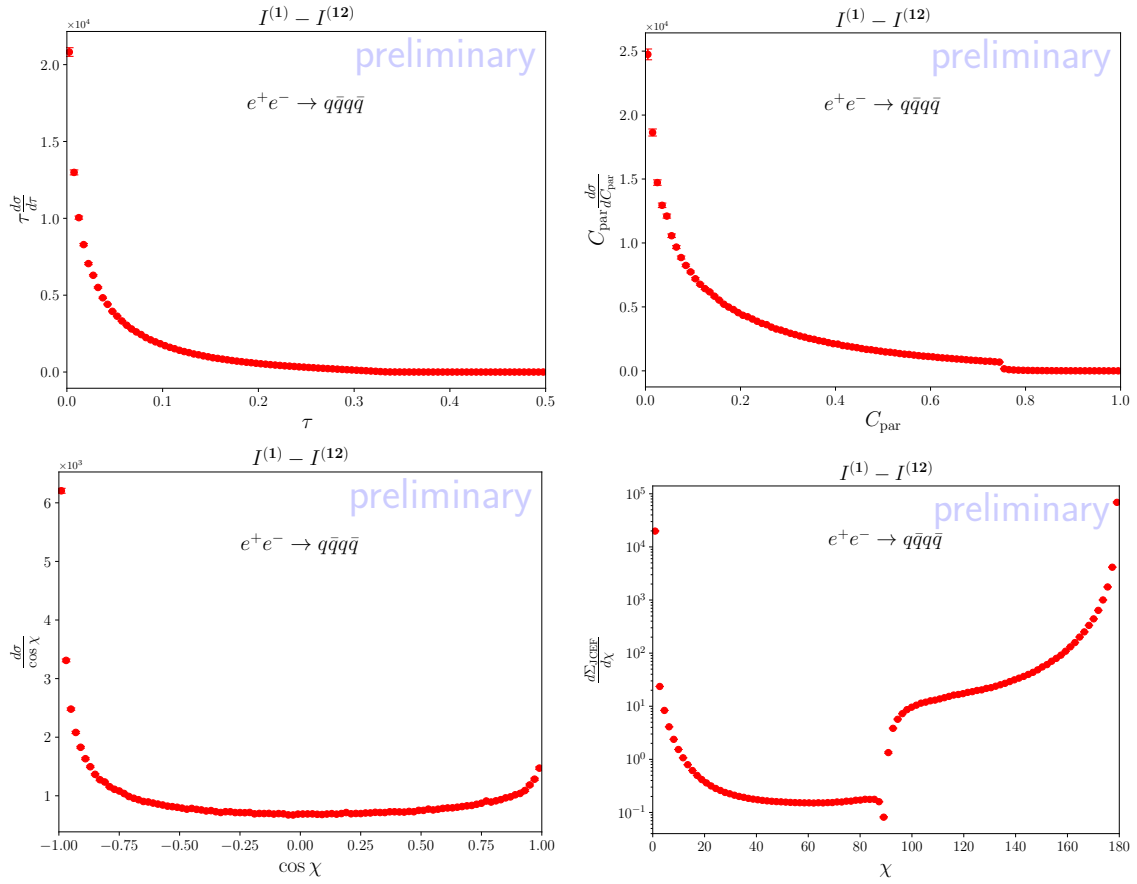


**Figure 3:** Real-virtual contributions to the (from left to right)  $\tau$ -parameter,  $C$ -parameter, energy-energy correlation and jet-cone energy fraction for  $e^+e^- \rightarrow q\bar{q}q\bar{q}$  from  $I^{(1)} - I^{(12)}$  terms.

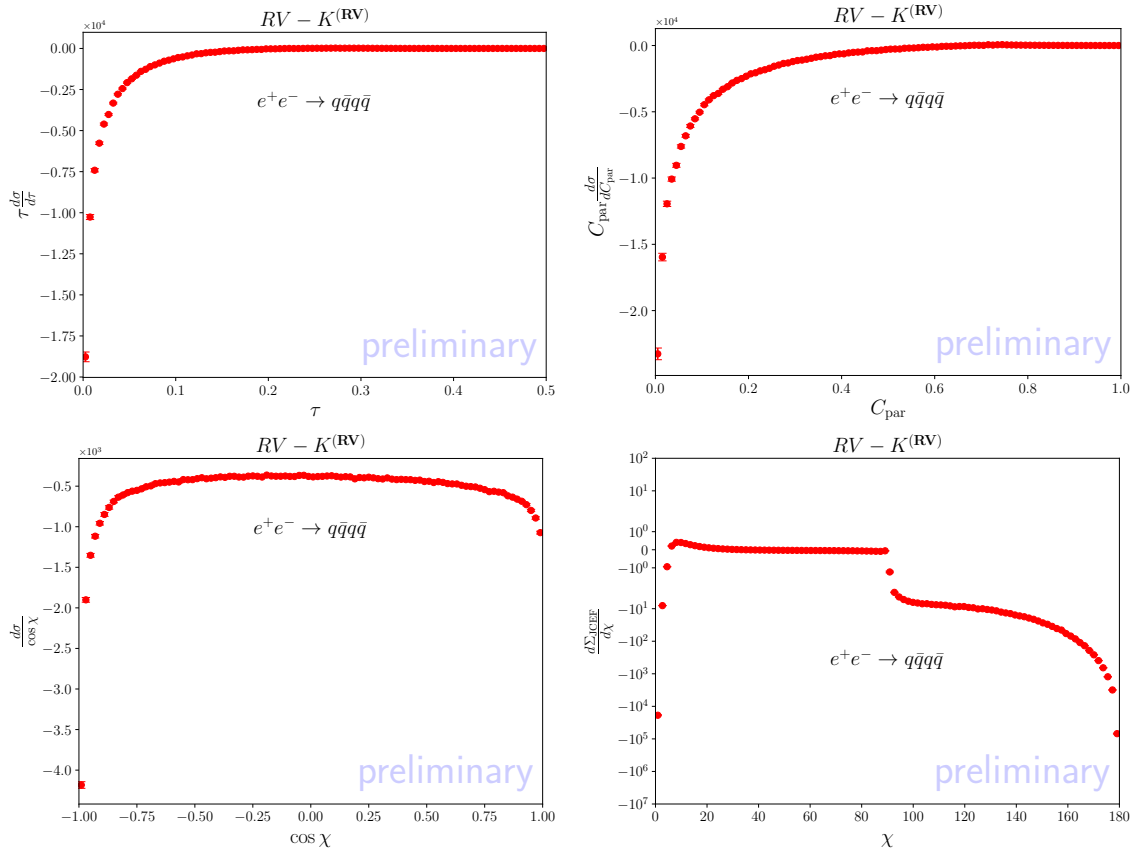


**Figure 4:** Real-virtual contributions to the (from left to right)  $\tau$ -parameter,  $C$ -parameter, energy-energy correlation and jet-cone energy fraction for  $e^+e^- \rightarrow q\bar{q}q\bar{q}$  from  $RV - K^{(RV)}$  terms.



## References

- [1] S. Frixione and M. Grazzini, *Subtraction at NNLO*, *JHEP* **06** (2005) 010 [[hep-ph/0411399](#)].
- [2] C. Anastasiou, K. Melnikov and F. Petriello, *A new method for real radiation at NNLO*, *Phys. Rev. D* **69** (2004) 076010 [[hep-ph/0311311](#)].
- [3] R. Boughezal, C. Focke, W. Giele, X. Liu and F. Petriello, *Higgs boson production in association with a jet at NNLO using jetiness subtraction*, *Phys. Lett. B* **748** (2015) 5 [[1505.03893](#)].
- [4] J. Gaunt, M. Stahlhofen, F.J. Tackmann and J.R. Walsh, *N-jettiness Subtractions for NNLO QCD Calculations*, *JHEP* **09** (2015) 058 [[1505.04794](#)].
- [5] A. Gehrmann-De Ridder, T. Gehrmann and E.W.N. Glover, *Antenna subtraction at NNLO*, *JHEP* **09** (2005) 056 [[hep-ph/0505111](#)].
- [6] J. Currie, E.W.N. Glover and S. Wells, *Infrared Structure at NNLO Using Antenna Subtraction*, *JHEP* **04** (2013) 066 [[1301.4693](#)].
- [7] G. Somogyi, Z. Trocsanyi and V. Del Duca, *Matching of singly- and doubly-unresolved limits of tree-level QCD squared matrix elements*, *JHEP* **06** (2005) 024 [[hep-ph/0502226](#)].
- [8] G. Somogyi, Z. Trocsanyi and V. Del Duca, *A Subtraction scheme for computing QCD jet cross sections at NNLO: Regularization of doubly-real emissions*, *JHEP* **01** (2007) 070 [[hep-ph/0609042](#)].
- [9] G. Somogyi and Z. Trocsanyi, *A Subtraction scheme for computing QCD jet cross sections at NNLO: Regularization of real-virtual emission*, *JHEP* **01** (2007) 052 [[hep-ph/0609043](#)].
- [10] F. Caola, K. Melnikov and R. Röntsch, *Nested soft-collinear subtractions in NNLO QCD computations*, *Eur. Phys. J. C* **77** (2017) 248 [[1702.01352](#)].
- [11] L. Magnea, E. Maina, G. Pelliccioli, C. Signorile-Signorile, P. Torrielli and S. Uccirati, *Local analytic sector subtraction at NNLO*, *JHEP* **12** (2018) 107 [[1806.09570](#)].
- [12] L. Magnea, G. Pelliccioli, C. Signorile-Signorile, P. Torrielli and S. Uccirati, *Analytic integration of soft and collinear radiation in factorised QCD cross sections at NNLO*, *JHEP* **02** (2021) 037 [[2010.14493](#)].
- [13] G. Bertolotti, L. Magnea, G. Pelliccioli, A. Ratti, C. Signorile-Signorile, P. Torrielli et al., *NNLO subtraction for any massless final state: a complete analytic expression*, *JHEP* **07** (2023) 140 [[2212.11190](#)].
- [14] A. Kardos, B. Chargeishvili, B. Giuseppe, S.-O. Moch and Z. Trocsanyi, *LASS, the numerics*, *PoS LL2024* (2024) .

- [15] S. Catani and M.H. Seymour, *A General algorithm for calculating jet cross-sections in NLO QCD*, *Nucl. Phys. B* **485** (1997) 291 [[hep-ph/9605323](#)].
- [16] N.K. Falck, D. Graudenz and G. Kramer, *Cross-section for Five Jet Production in  $e^+e^-$  Annihilation*, *Nucl. Phys. B* **328** (1989) 317.
- [17] K. Hagiwara and D. Zeppenfeld, *Amplitudes for Multiparton Processes Involving a Current at  $e^+e^-$ ,  $e^+p$ , and Hadron Colliders*, *Nucl. Phys. B* **313** (1989) 560.
- [18] F.A. Berends, W.T. Giele and H. Kuijf, *Exact Expressions for Processes Involving a Vector Boson and Up to Five Partons*, *Nucl. Phys. B* **321** (1989) 39.
- [19] Z. Bern, L.J. Dixon and D.A. Kosower, *One loop corrections to five gluon amplitudes*, *Phys. Rev. Lett.* **70** (1993) 2677 [[hep-ph/9302280](#)].
- [20] L.W. Garland, T. Gehrmann, E.W.N. Glover, A. Koukoutsakis and E. Remiddi, *The Two loop QCD matrix element for  $e^+e^- \rightarrow 3$  jets*, *Nucl. Phys. B* **627** (2002) 107 [[hep-ph/0112081](#)].
- [21] A. Gehrmann-De Ridder, T. Gehrmann, E.W.N. Glover and G. Heinrich, *NNLO corrections to event shapes in  $e^+e^-$  annihilation*, *JHEP* **12** (2007) 094 [[0711.4711](#)].
- [22] G.P. Lepage, *Adaptive multidimensional integration: VEGAS enhanced*, *J. Comput. Phys.* **439** (2021) 110386 [[2009.05112](#)].
- [23] V. Del Duca, C. Duhr, A. Kardos, G. Somogyi and Z. Trócsányi, *Three-Jet Production in Electron-Positron Collisions at Next-to-Next-to-Leading Order Accuracy*, *Phys. Rev. Lett.* **117** (2016) 152004 [[1603.08927](#)].
- [24] S. Weinzierl, *Event shapes and jet rates in electron-positron annihilation at NNLO*, *JHEP* **06** (2009) 041 [[0904.1077](#)].
- [25] A. Kardos, A. Larkoski and Z. Trócsányi, *Soft-Dropped Observables with CoLoRFuLNNLO*, *Acta Phys. Polon. B* **50** (2019) 1891.